DRAFT: DO NOT CITE OR QUOTE

Draft for open comment

Tropospheric Ozone Assessment Report: Present-day distribution and trends of tropospheric ozone relevant to climate and global atmospheric chemistry model evaluation

Author Team: A. Gaudel, O. R. Cooper, G. Ancellet, B. Barret, A. Boynard, J. P. Burrows, C. Clerbaux, P.-F. Coheur, J. Cuesta, E. Cuevas, S. Doniki, G. Dufour, F. Ebojie, G. Foret, O. Garcia, M. J. Granados-Muñoz, J. Hannigan, F. Hase, B. Hassler, G. Huang, D. Hurtmans, D. Jaffe, N. Jones, P. Kalabokas, B. Kerridge, S. Kulawik, B. Latter, T. Leblanc, E. Le Flochmoën, W. Lin, J. Liu, X. Liu, E. Mahieu, A. McClure-Begley, J. L. Neu, M. Osman, M. Palm, H. Petetin, I. Petropavlovskikh, R. Querel, N. Rahpoe, A. Rozanov, M. G. Schultz, J. Schwab, R. Siddans, D. Smale, M. Steinbacher, H. Tanimoto, D. Tarasick, V. Thouret, A. M. Thompson, T. Trickl, E. Weatherhead, C. Wespes, H. Worden, C. Vigouroux, X. Xu, G. Zeng, J. Ziemke

The Tropospheric Ozone Assessment Report (TOAR) is a current IGAC activity (http://www.igacproject.org/activities/TOAR) with a mission to provide the research community with an up-to-date scientific assessment of tropospheric ozone's global distribution and trends from the surface to the tropopause.

Guided by this mission, TOAR has two goals:

1) Produce the first tropospheric ozone assessment report based on the peer-reviewed literature and new analyses.

2) Generate easily accessible, documented data on ozone exposure and dose metrics at hundreds of measurement sites around the world (urban and non-urban), freely accessible for research on the global-scale impact of ozone on climate, human health and crop/ecosystem productivity.

The report is being written as a series of eight stand-alone publications to be submitted for peer-review to *Elementa: Science of the Anthropocene*, an open-access, non-profit science journal founded by five US research Universities and published by University of California Press (www.elementascience.org). Prior to submission each paper will be posted to the TOAR webpage (http://www.igacproject.org/activities/TOAR/OpenComments) for a 30-day open comment period. We invite members of the atmospheric and biological sciences communities as well as the general public to read the papers and provide comments if they wish to do so. The open comment period will last for 30 days for each paper, with the draft papers posted to the website as they become available.

To provide comments on this particular paper, please send an e-mail to lead author Audrey Gaudel: Audrey.Gaudel@colorado.edu

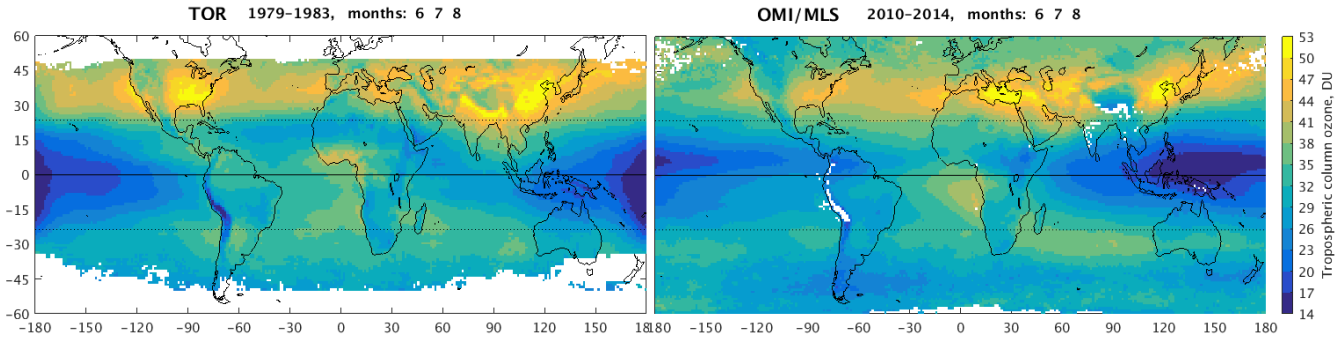

Figure 4.3.1 June-July-August TCO as measured by the TOR product for 1979-1983 (left) and OMI/MLS for 2010-2014 (right).

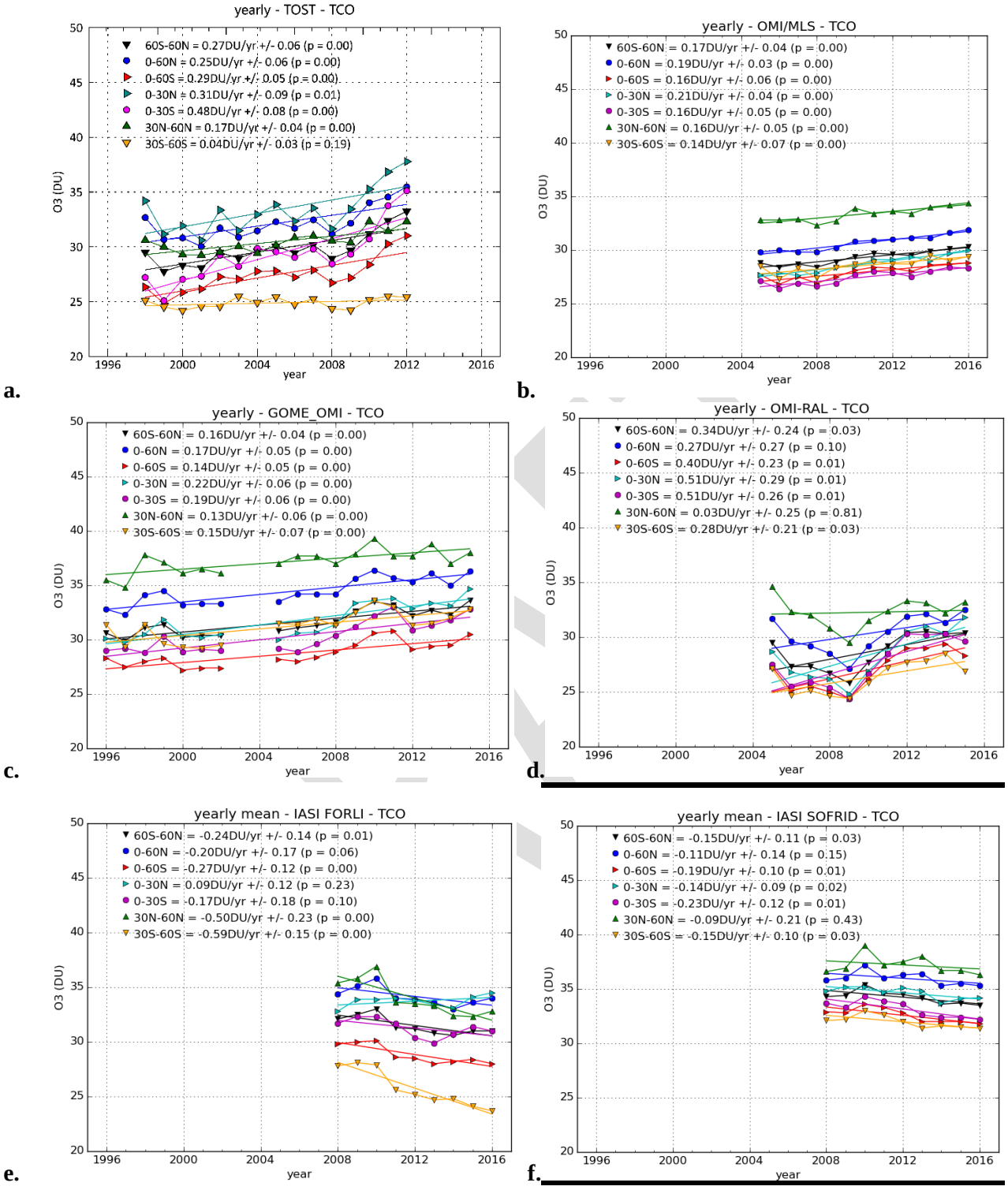

Figure 4.3.2 TCO (surface to tropopause) by latitude band (60°N-60°S, 0-60°N, 0-60°S, 0-30°N, 0-30°S, 30-60°N, 30-60°S) as measured by (a) TOST, (b) OMI/MLS, (c) GOME/OMI-SAO, (d) OMI-RAL, (e) IASI-FORLI, and (f) IASI-SOFRID. Linear trends are reported with 95% confidence intervals and p-values.

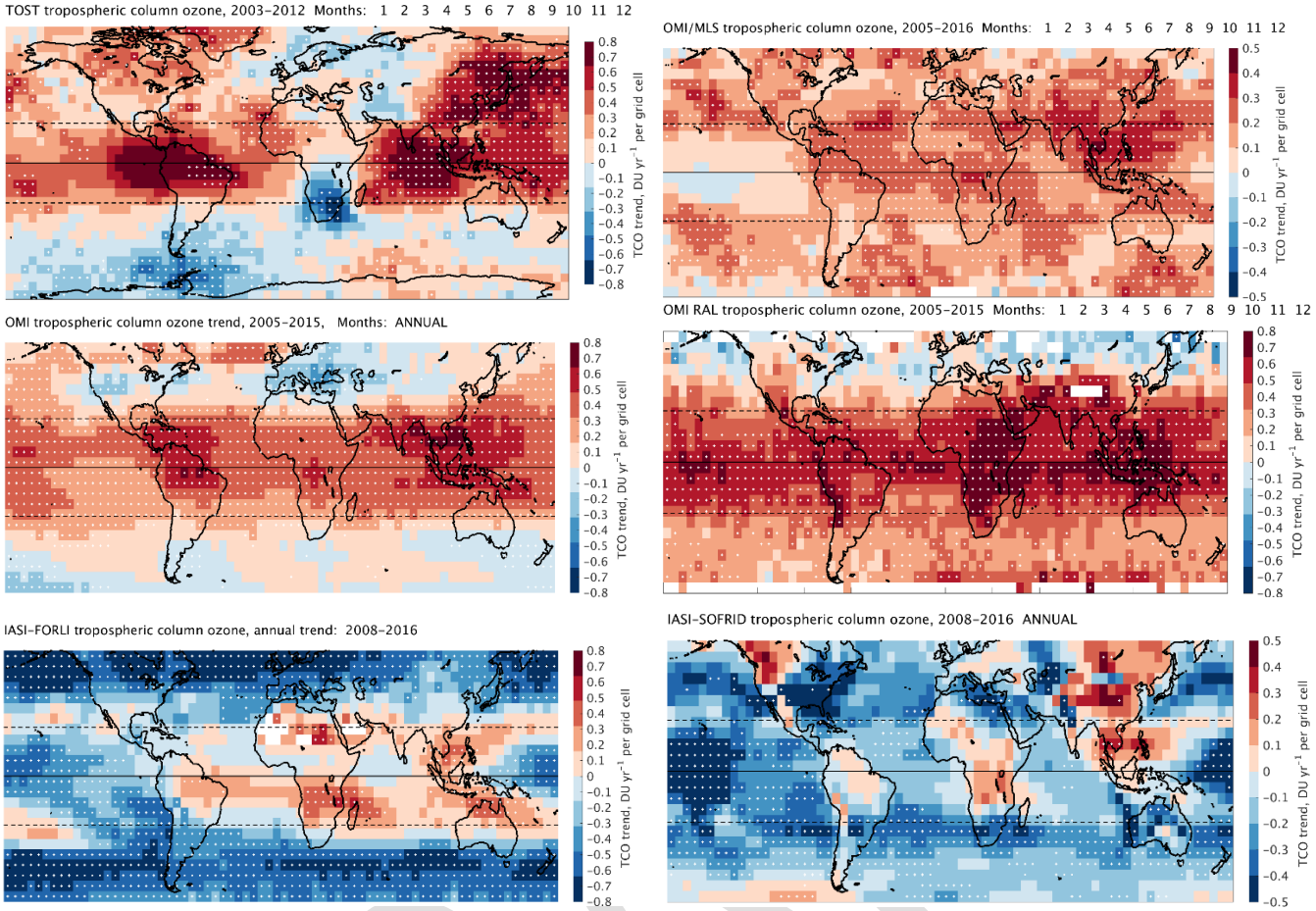

Figure 4.3.3 (top left) 2003-2012 TOST ozonesonde annual TCO trends for each 5° x 5° grid cell between 80° S – 80° N. White dots indicate grid cells with statistically significant trends. Also shown are satellite products between 60° S – 60° N: (top right) OMI/MLS, 2005-2016, (middle left) OMI-SAO, 2005-2016, (middle right) OMI-RAL, 2005-2015, (bottom left) IASI-FORLI, 2008-2016, and (bottom right) IASI-SOFRID, 2008-2015. Note that OMI/MLS and IASI-SOFRID have different color scales from the rest. Trends in this figure are based on least-squares linear regression and reported with 95% confidence intervals and p-values.

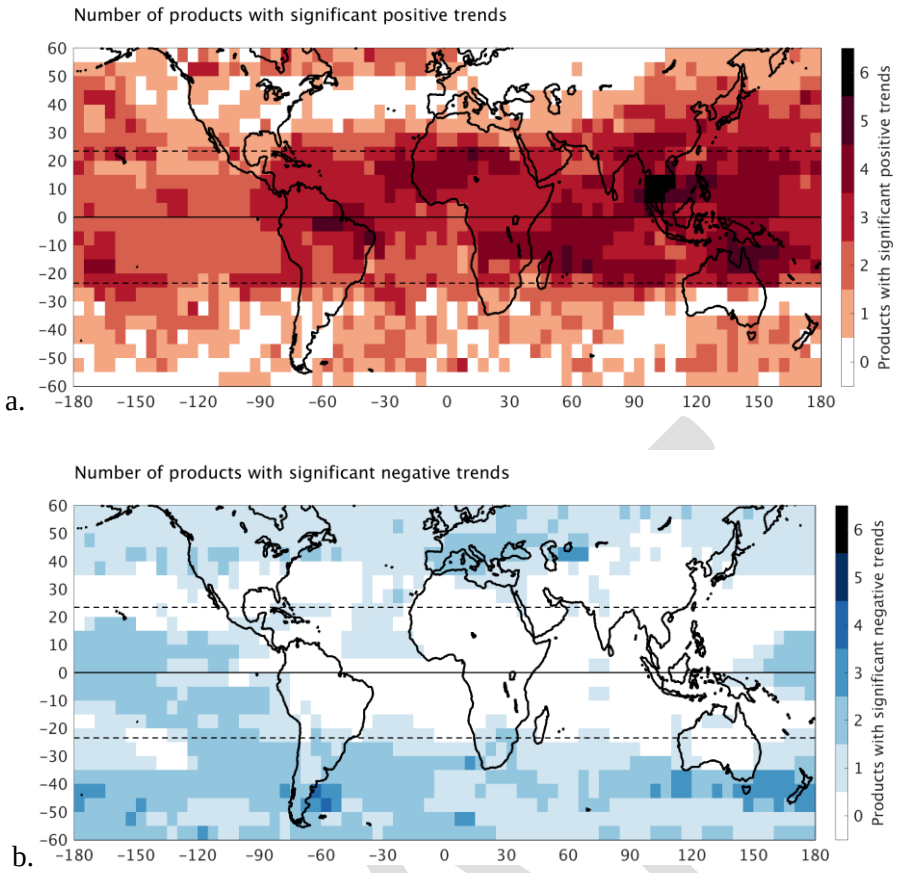

Figure 4.3.4 (a) Number of products from Figure 4.3.3 that indicate a statistically significant positive trend in each 5° x 5° grid cell. All six products shows significant ozone increases in five grid cells, all above Southeast Asia. (b) As in (a) but for statistically significant negative trends.

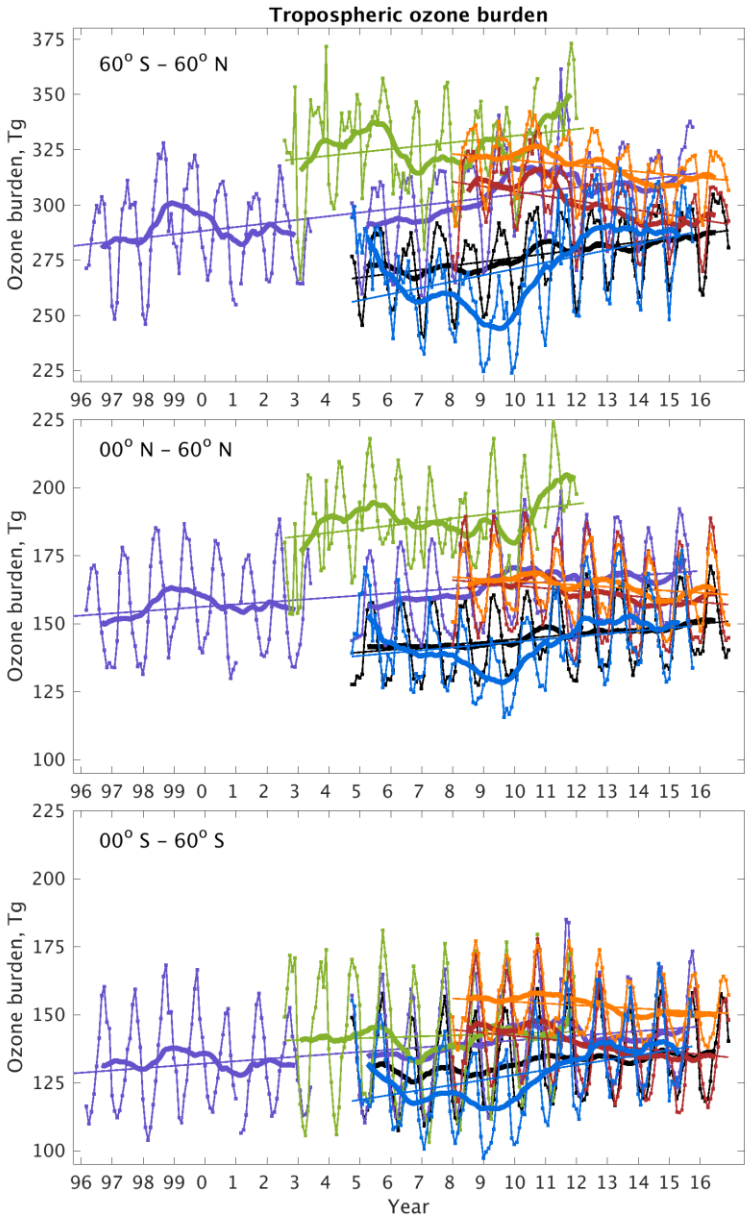

	change, Tg yr^{-1}	p-value
Black: OMI/MLS	1.79 +/- 0.66	0.00
Brown: IASI-FORLI	-2.15 +/- 1.03	0.00
Orange: IASI-SOFRID	-1.34 +/- 0.92	0.00
Purple: GOME/OMI	1.63 +/- 0.45	0.00
Blue: OMI-RAL	2.85 +/- 1.16	0.00
Green: SCIAMACHY	1.50 +/- 1.39	0.03

	change, Tg yr^{-1}	p-value
Black: OMI/MLS	0.95 +/- 0.55	0.00
Brown: IASI-FORLI	-1.01 +/- 1.17	0.09
Orange: IASI-SOFRID	-0.73 +/- 0.81	0.08
Purple: GOME/OMI	0.82 +/- 0.35	0.00
Blue: OMI-RAL	1.02 +/- 0.79	0.01
Green: SCIAMACHY	1.33 +/- 1.04	0.01

	change, Tg yr^{-1}	p-value
Black: OMI/MLS	0.83 +/- 0.64	0.01
Brown: IASI-FORLI	-1.14 +/- 1.14	0.05
Orange: IASI-SOFRID	-0.61 +/- 0.80	0.14
Purple: GOME/OMI	0.85 +/- 0.39	0.00
Blue: OMI-RAL	1.83 +/- 0.84	0.00
Green: SCIAMACHY	0.34 +/- 1.48	0.65

Figure 5.7.1 Monthly tropospheric ozone burden (thin curves) for 60° S - 60° N (top), 00° N - 60° N (middle), and 00° S - 60° S (bottom), for six different satellite products. Thick curves are the 12-month running means and the thin straight lines are the least square linear fits. Trends in this figure are based on least-squares linear regression and reported with 95% confidence intervals and p-values.

SUPPLEMENTARY FIGURES

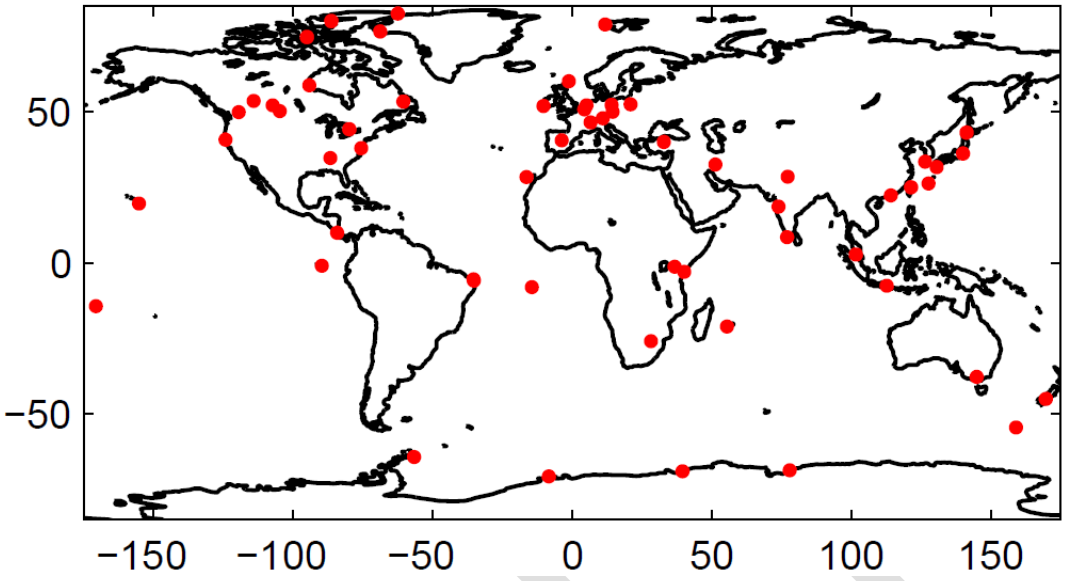

Figure S2.3.2. Locations of the ozonesonde stations used in the TOST product for the period 2008-2012.

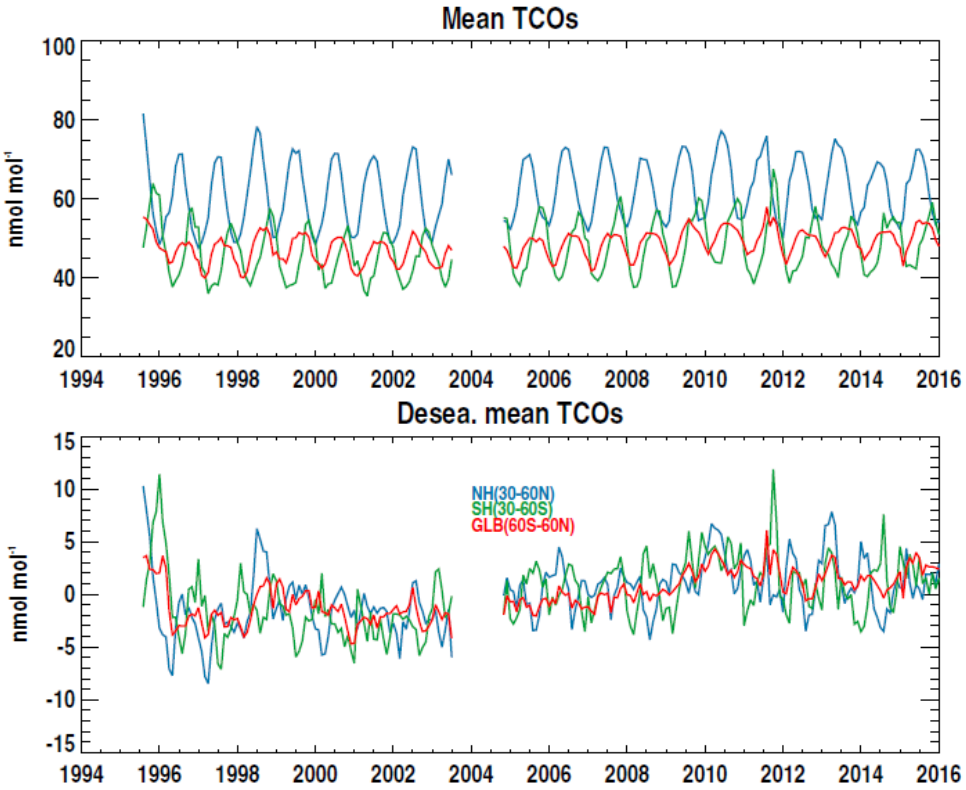

Figure S2.4.2. Time series of GOME and OMI monthly mean tropospheric ozone mole fractions (converted from TCO) averaged over 30°N-60°N, 30°S-30°N, 60°S-30°S, respectively, and their corresponding de-seasonalized values after subtracting average values over all the data for each individual month.

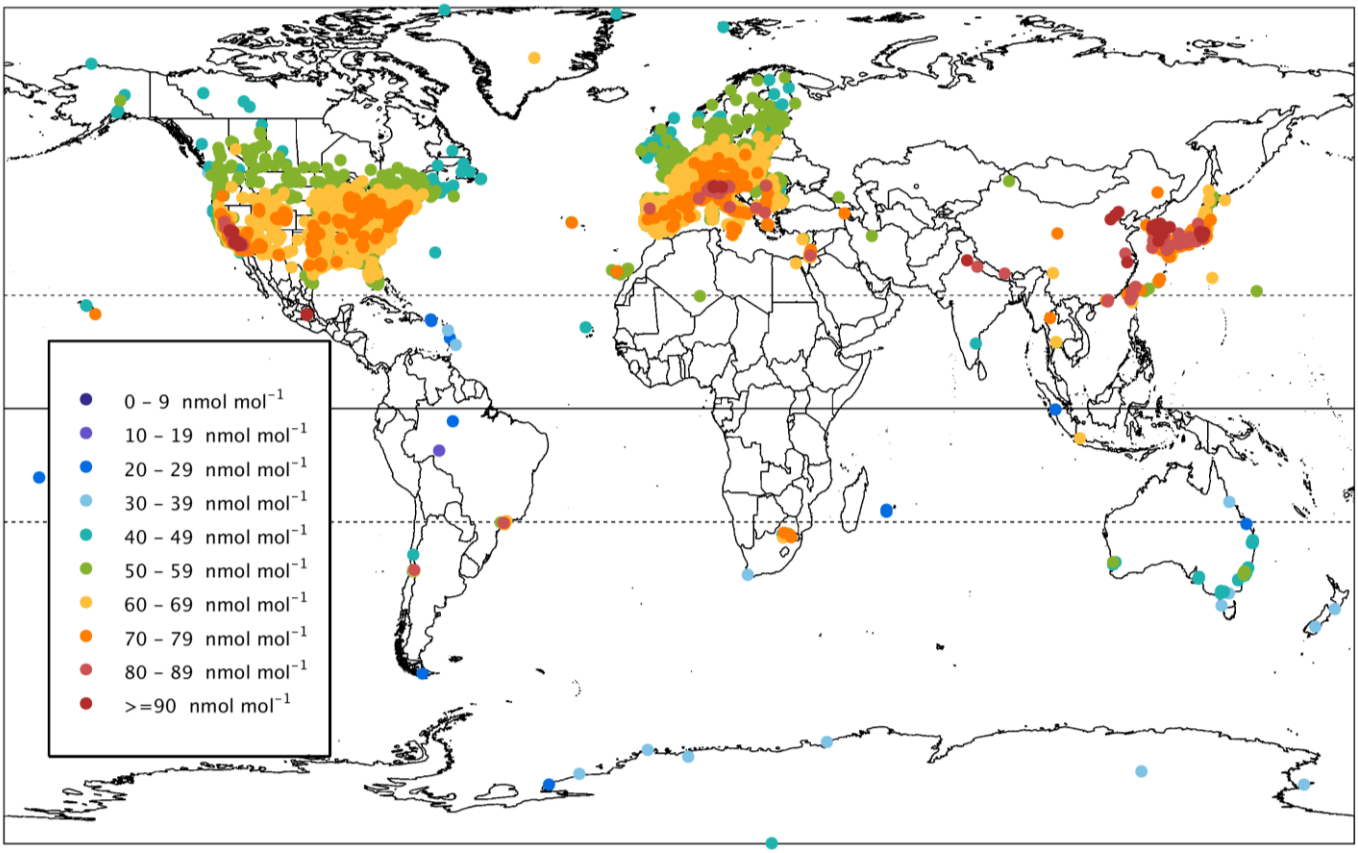

Figure S3.1. 98th percentile ozone (nmol mol^{-1}) at all available surface sites (4792 sites) for the warm season (April-September in the Northern Hemisphere, and October-March in the Southern Hemisphere) for the present-day period, 2010-2014.

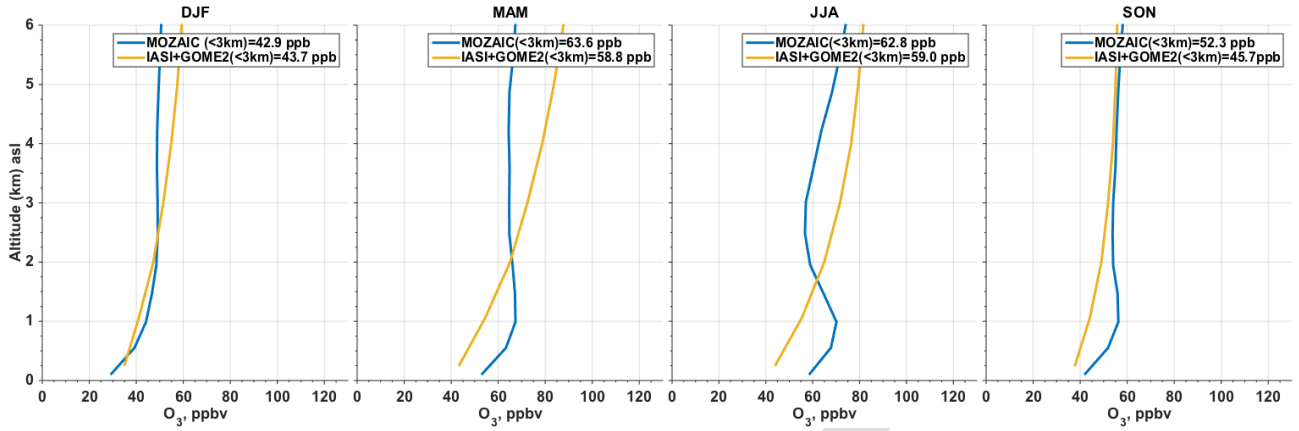

Figure S3.3. Comparison between MOZAIC/IAGOS (2005-2014) and IASI+GOME2 (2010) for the region 30-43°N 110-129°E (confined to the land areas of eastern China and South Korea).

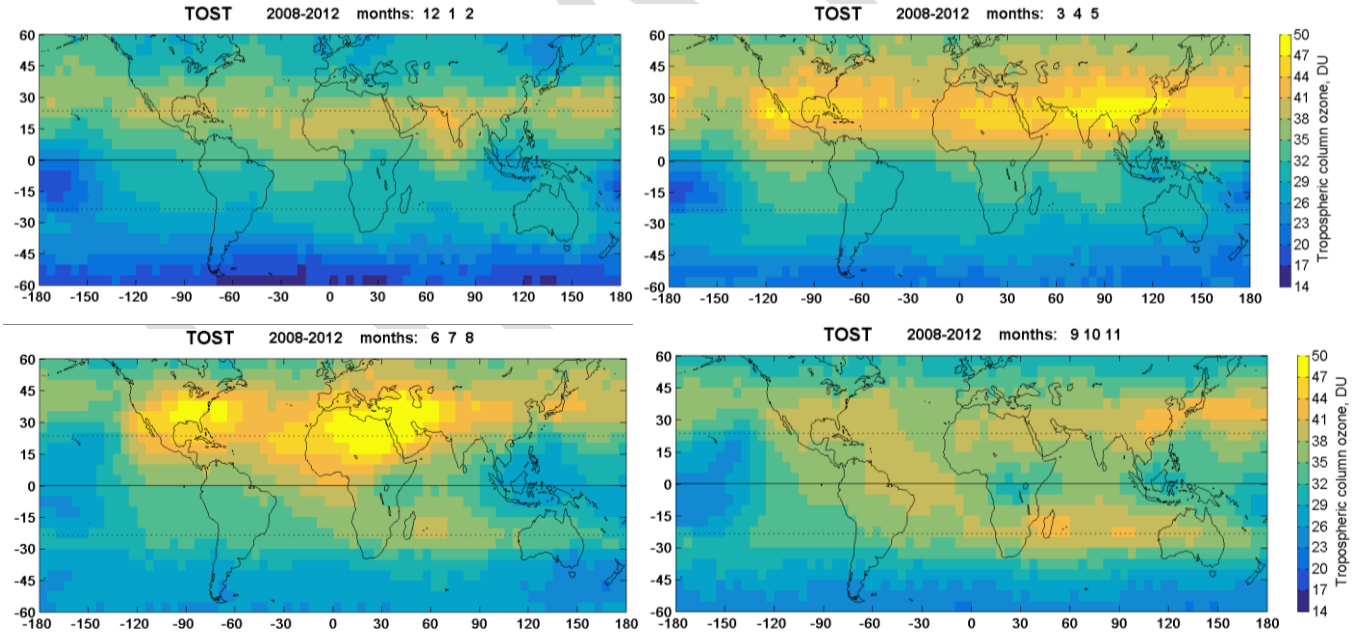

Figure S3.4.1. TOST 2008-2012 tropospheric column ozone (DU) for winter (DJF), spring (MAM), summer (JJA) and fall (SON).

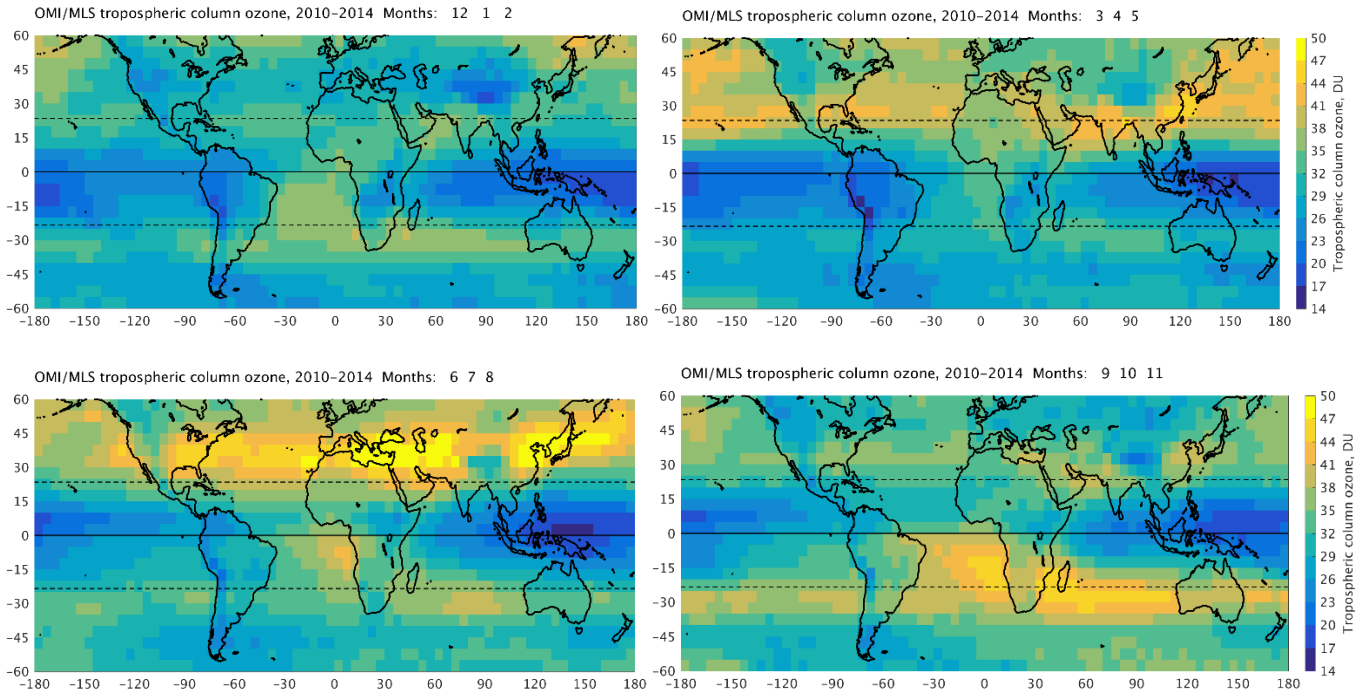

Figure S3.4.2. OMI/MLS tropospheric column ozone (DU) by season. The data are averaged over the period January 2010 – December 2014 and reported at 5° × 5° horizontal resolution. A uniform value of 2 DU was added to each grid cell to offset the product's low bias.

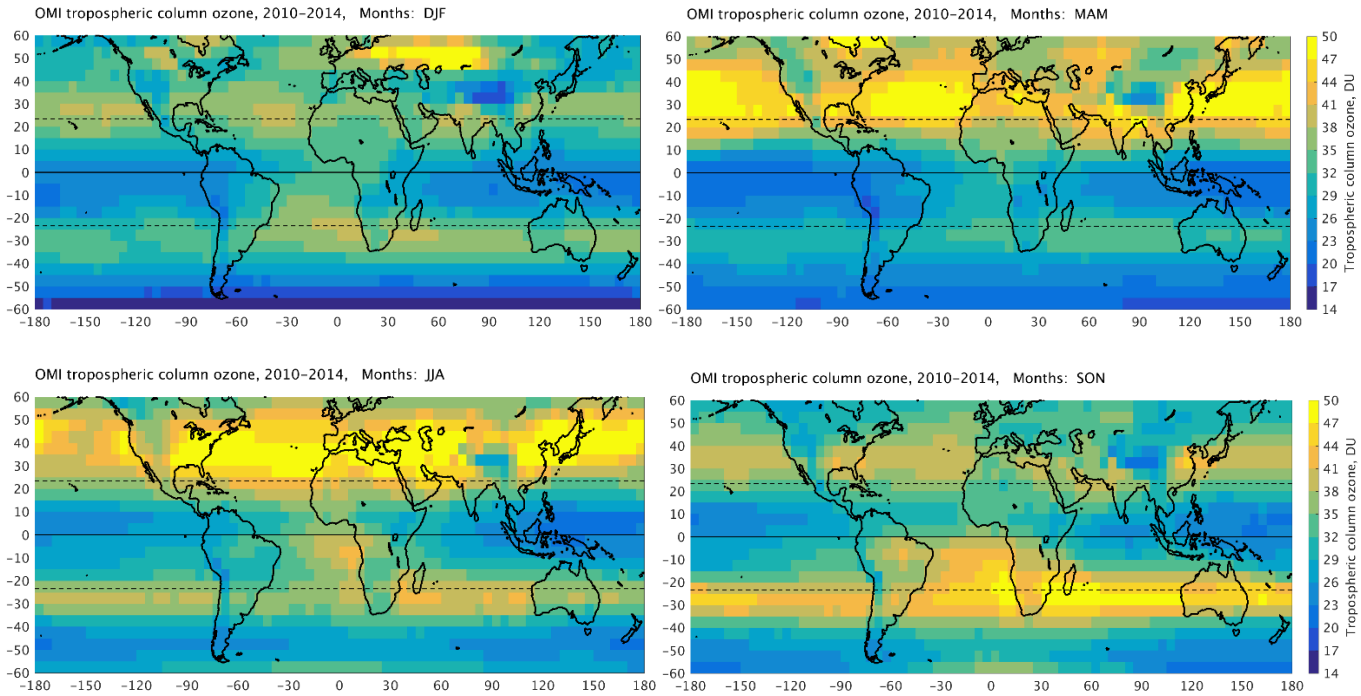

Figure S3.4.3. OMI-SAO tropospheric column ozone (DU) by season. The data are averaged over the period January 2010 through December 2014 and reported at 5° x 5° horizontal resolution.

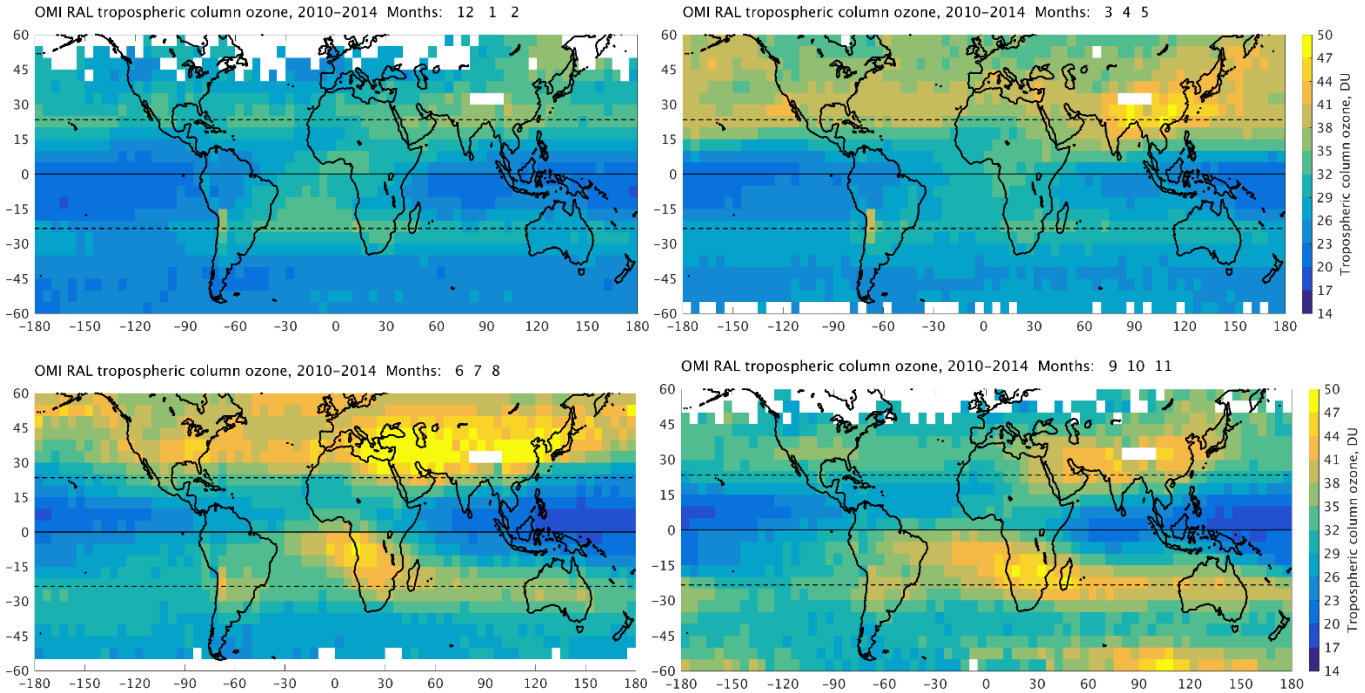

Figure S3.4.4. OMI-RAL tropospheric column ozone (DU) by season. The data are averaged over the period January 2010 through December 2014 and reported at 5° x 5° horizontal resolution.

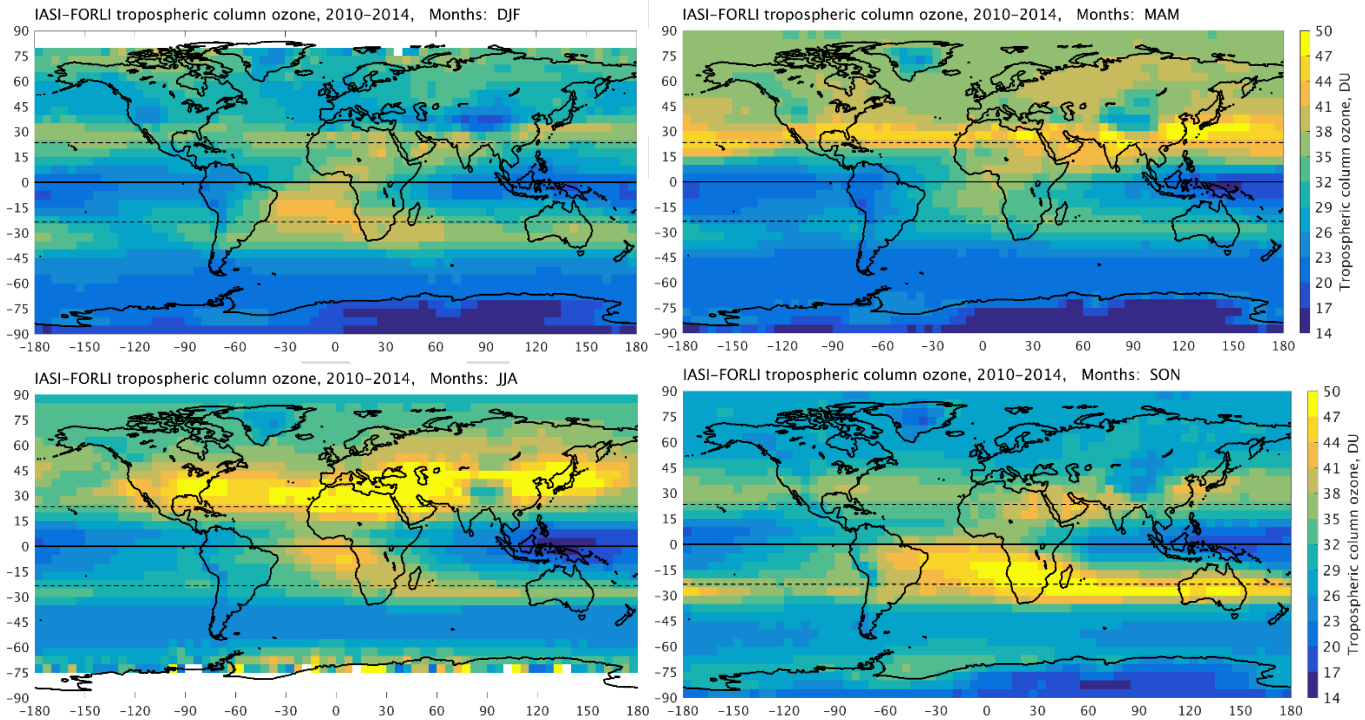

Figure S3.4.5. IASI-FORLI tropospheric column ozone (DU) by season. The data are averaged over the period January 2010 through December 2014 and reported at 5°×5° horizontal resolution.

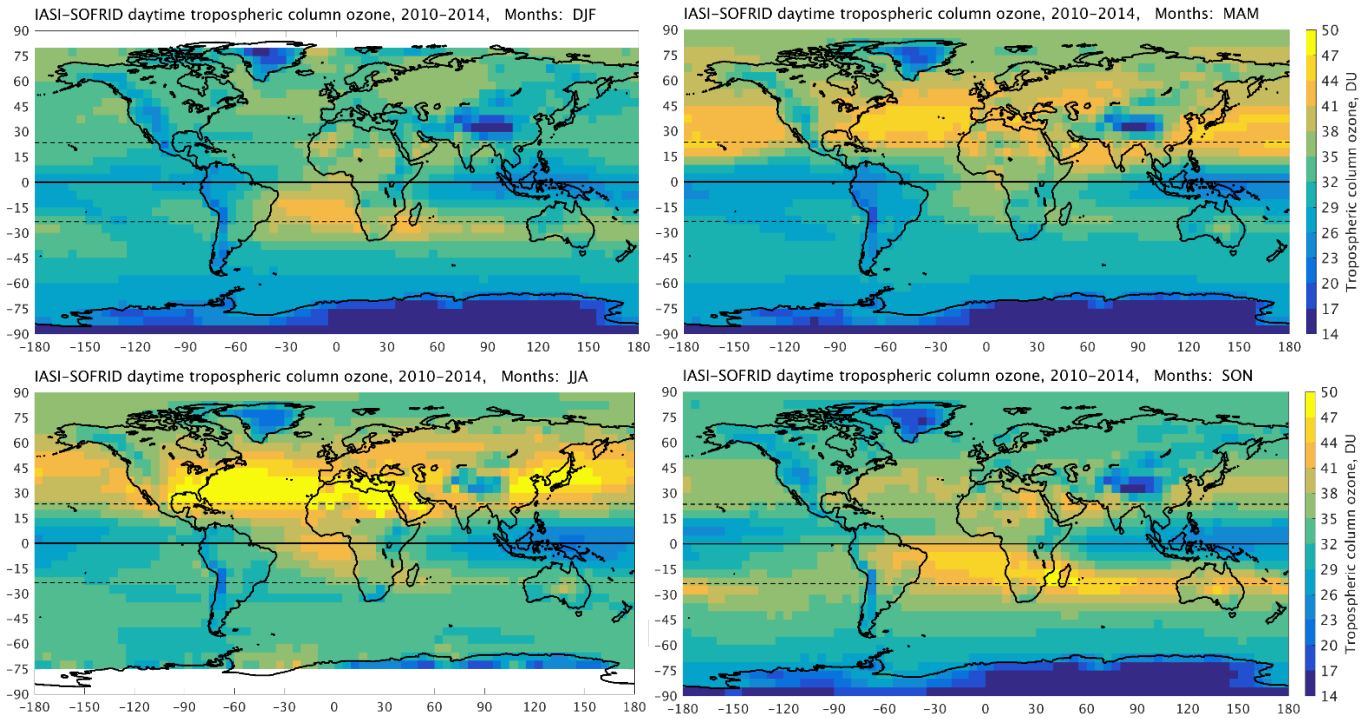

Figure S3.4.6. IASI-SOFRID tropospheric column ozone (DU) by season. The data are averaged over the period January 2010 through December 2014 and reported at 5°×5° horizontal resolution.

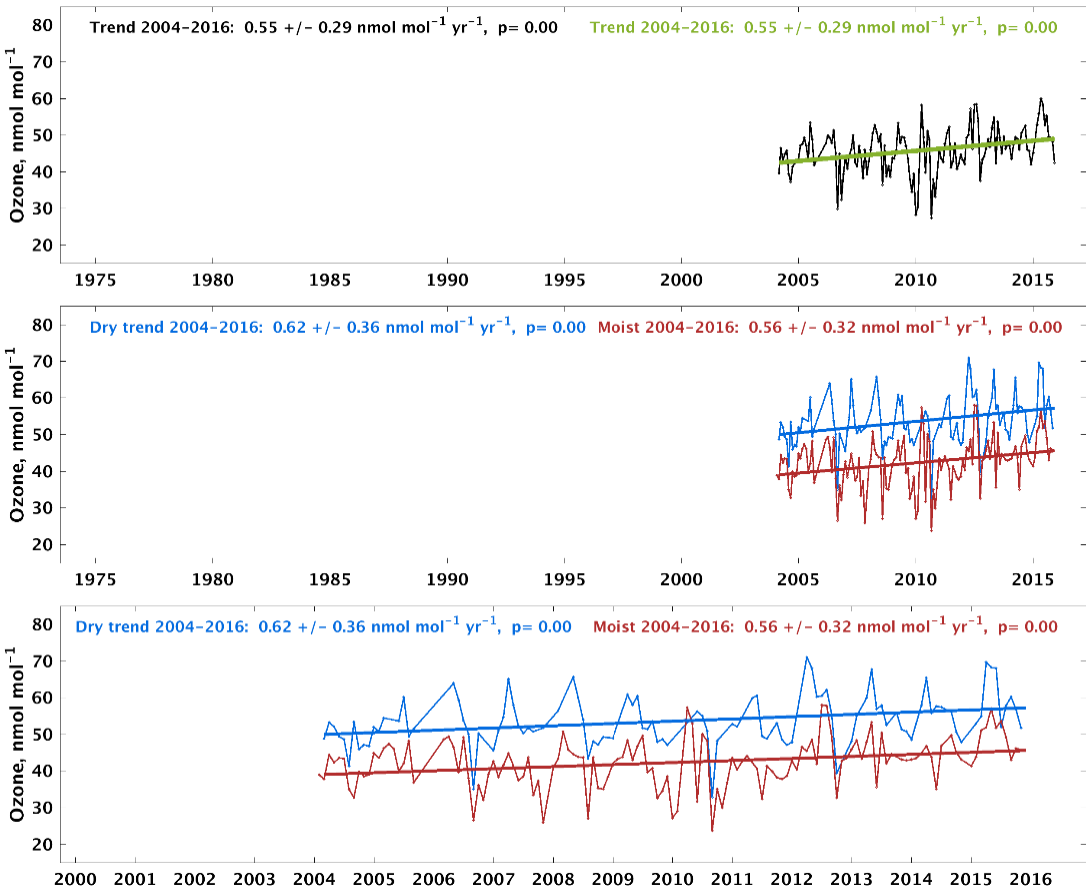

Figure S.4.1.1. a) Nighttime monthly median ozone values at Mt. Bachelor Observatory for months with at least 50% data availability, February 2004 – December 2015. b) Same as in a) but for data split into dry (dewpoint less than the monthly 40th percentile and relative humidity < 80%) and moist (dewpoint greater than the monthly 60th percentile) categories. A monthly sample size of at least 24 individual hourly nighttime observations is required. c) As in b) but with expanded x-axis. Trends in this figure are based on least-squares linear regression fit through the monthly median values, and reported with 95% confidence intervals and p-values.

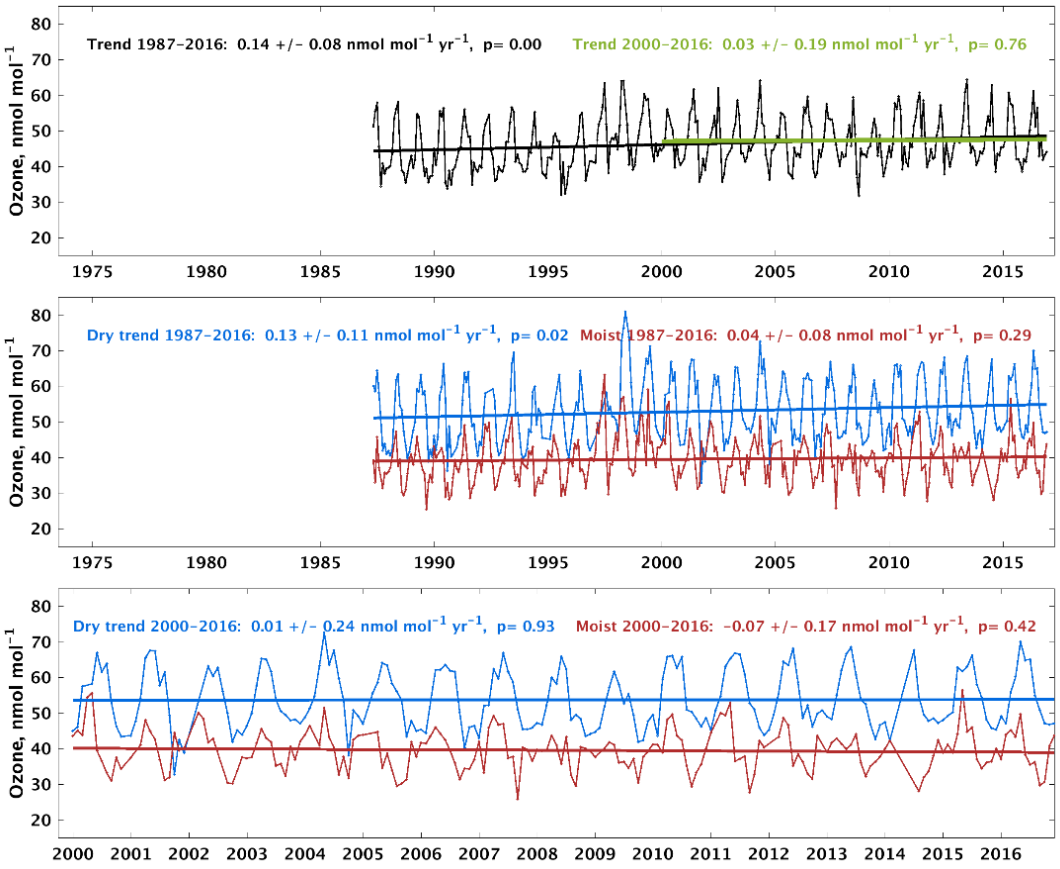

Figure S.4.1.2. a) Nighttime monthly median ozone values at Izaña for months with at least 50% data availability, May 1987 – December 2013. b) Same as in a) but for data split into dry (dewpoint less than the monthly 40th percentile) and moist (dewpoint greater than the monthly 60th percentile) categories. A monthly sample size of at least 24 individual hourly nighttime observations is required. c) As in b) but with expanded x-axis. Trends in this figure are based on least-squares linear regression fit through the monthly median values, and reported with 95% confidence intervals and p-values.

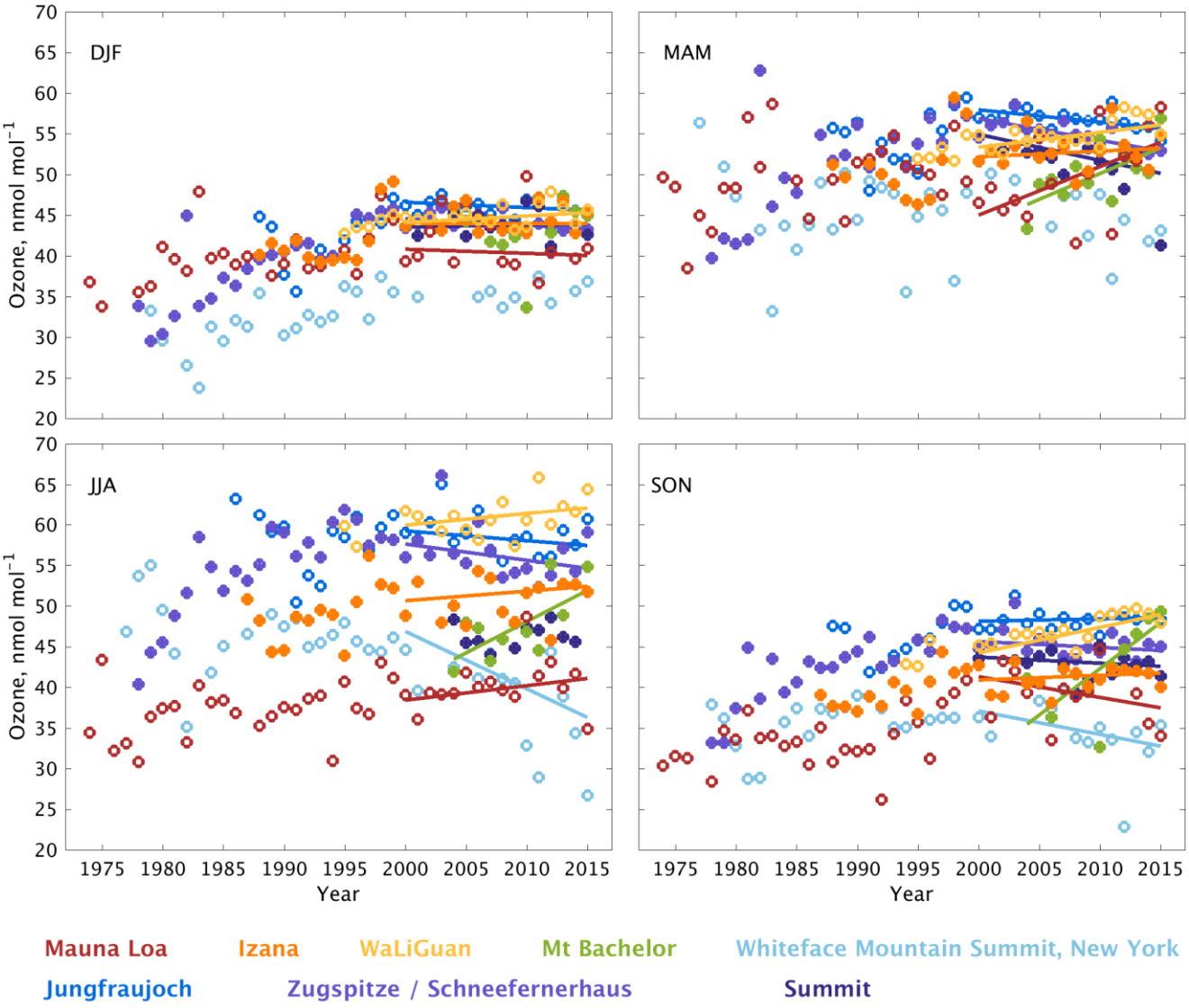

Figure S.4.1.3. Nighttime ozone trends (2000-2015) at eight Northern Hemisphere mountaintop sites by season. Trend values are given in Table 4.1.

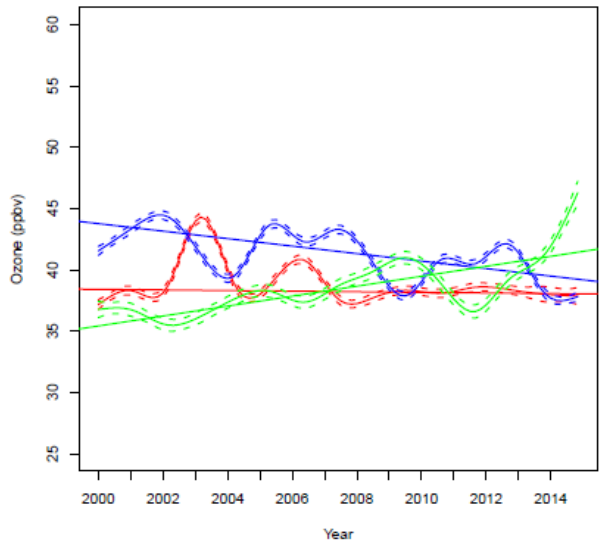

(a) $f_2(interannual)$: Daytime average trends

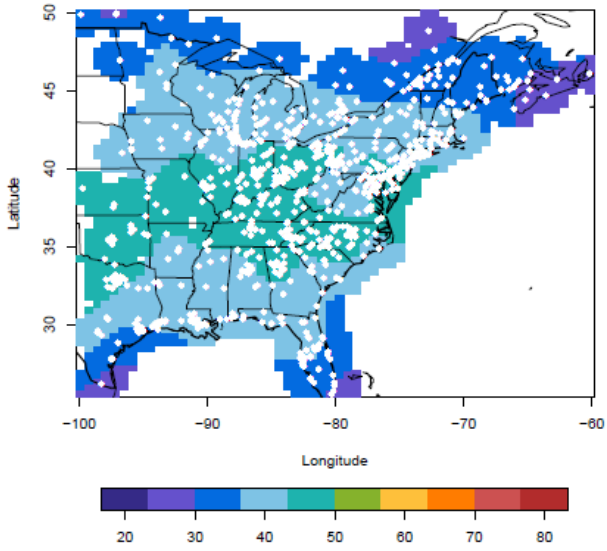

(b) $f_3(spatial)$: Eastern North America

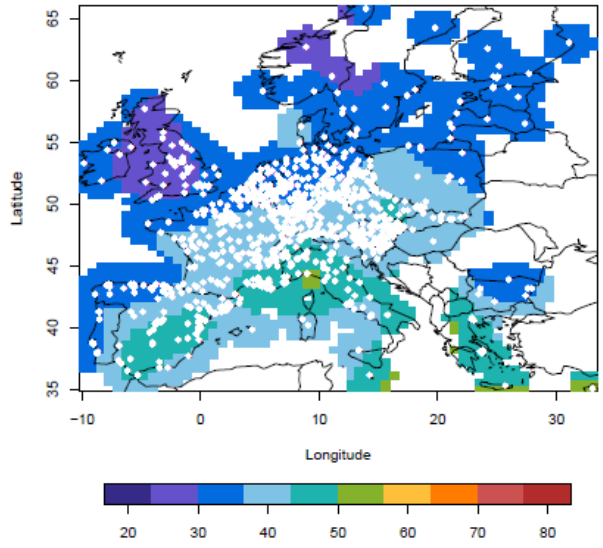

(c) $f_3(spatial)$: Europe

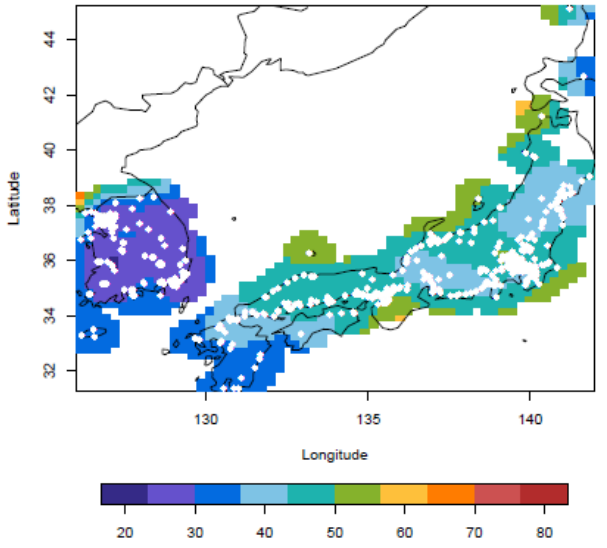

(d) $f_3(spatial)$: East Asia

Figure S.4.1.4. a) Regional trends (2000-2014) of summertime (April-September) daytime average ozone across eastern North American (blue), Europe (red) and east Asia (green), and their spatial effects (b, c, d) in the generalized additive mixed model (GAMM) analysis (Chang et al., 2017). *f*2(interannual) and *f*3(spatial) refer to terms in the generalized additive mixed model, as described by Chang et al., 2017. The white points indicate the locations of the ozone monitoring stations.

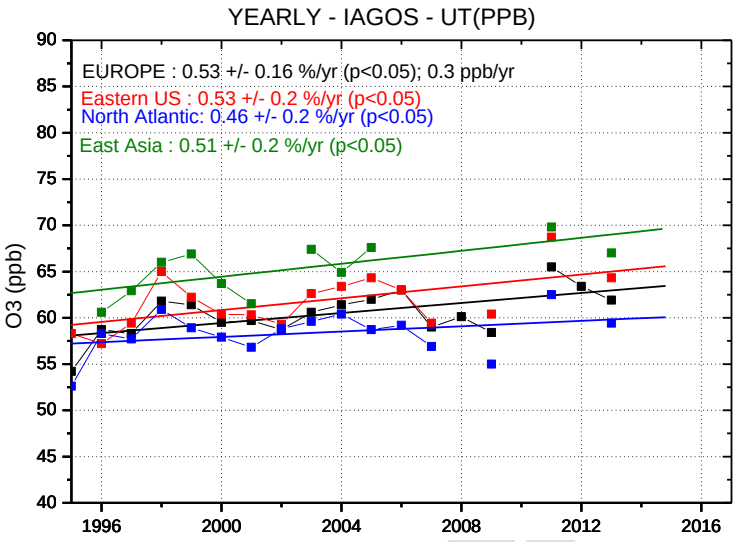

Figure S4.2.1. Upper tropospheric ozone trends as measured by MOZAIC/IAGOS, 1995-2013. Figure provided by Y. Cohen and V. Thouret, based on results from *Cohen et al., 2017*.

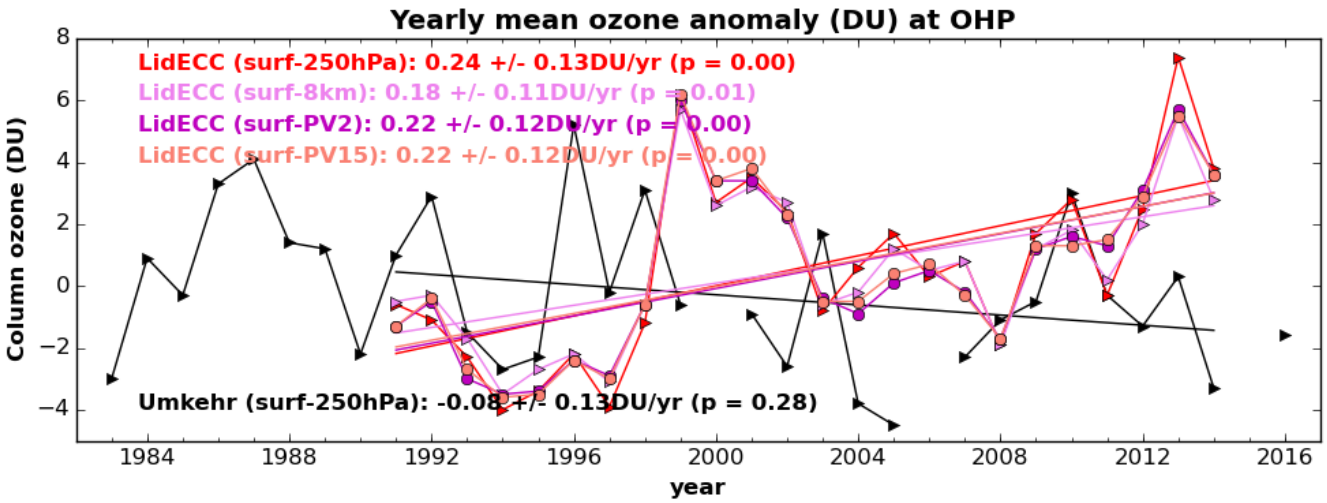

Figure S4.2.2. Comparison of annual ozone anomalies (tropospheric ozone columns in Dobson units) as measured by Umkehr and Lidar/ECC combined above Observatoire de Haute Provence (OHP), France. Ozone columns extend from the surface to 8 km, 250 hPa or the dynamical tropopause defined with the iso-potential vorticity (PV) at 2 or 1.5 PVu, as labeled in the figure. Trends in this figure are based on least-squares linear regression and reported with 95% confidence intervals and p-values.

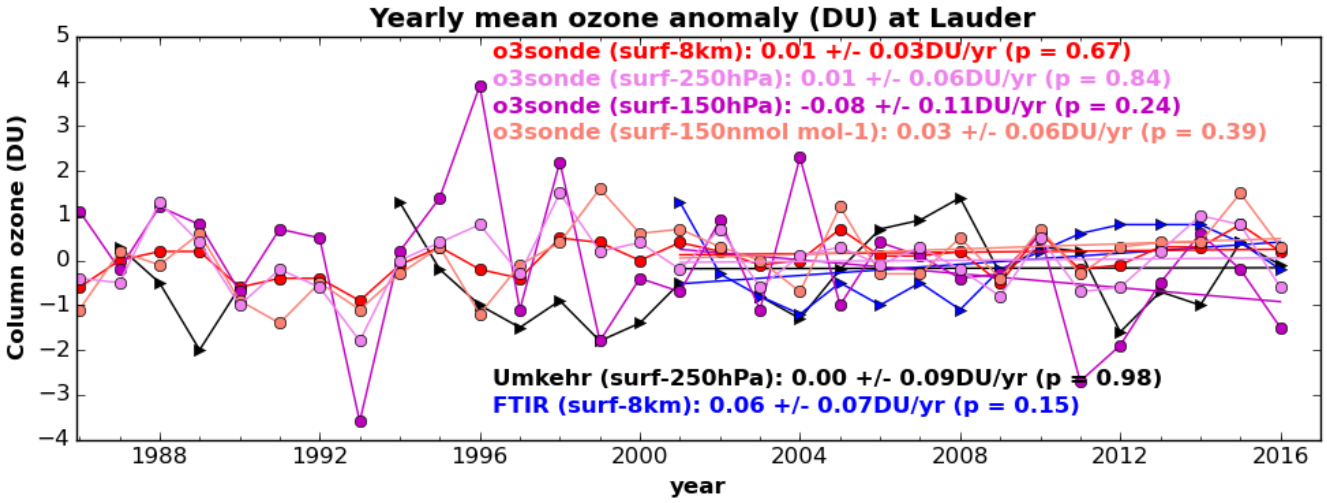

Figure S4.2.3. Comparison of annual ozone anomalies (tropospheric ozone columns in Dobson units) as measured by FTIR, Umkehr and ozonsondes above Lauder, New Zealand. Ozone columns extend from the surface to 8 km, 250 hPa or to the 150 nmol mol^{-1} ozone isosurface, as labeled in the figure. Trends in this figure are based on least-squares linear regression and reported with 95% confidence intervals and p-values.

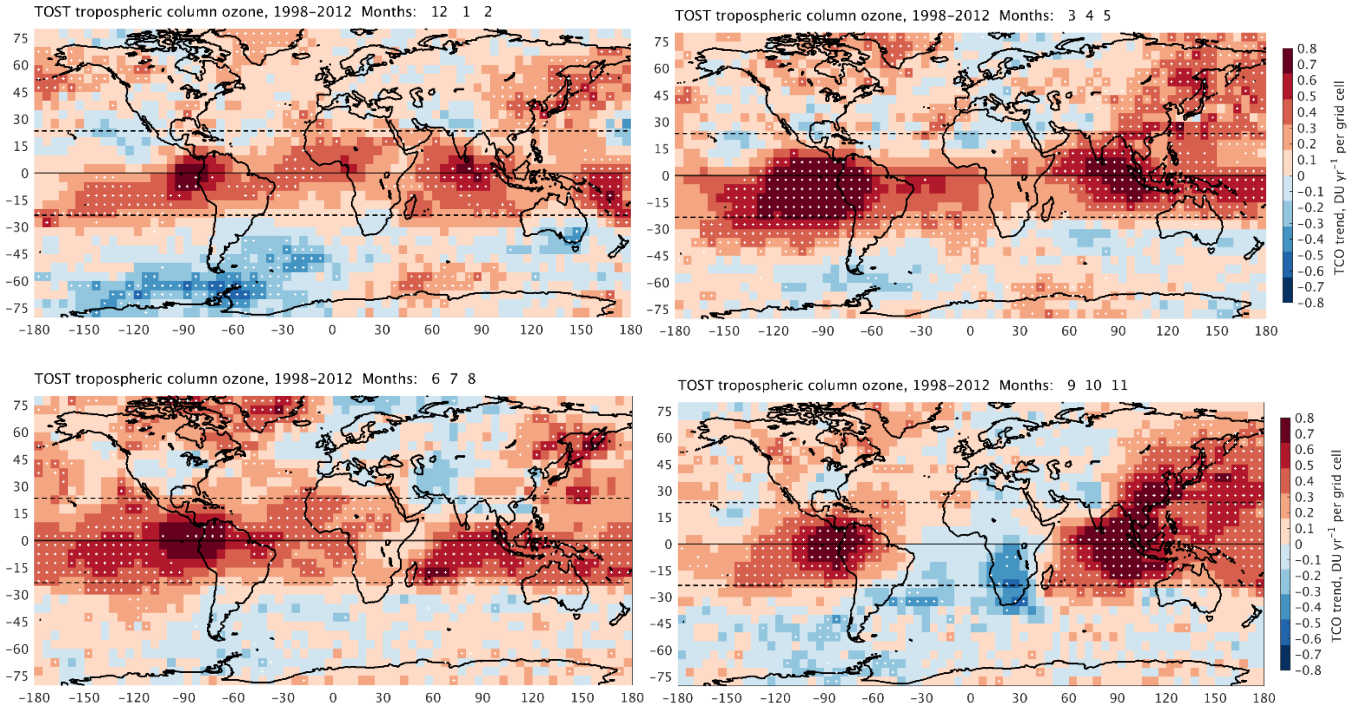

Figure S4.3.1. 1998-2012 TOST TCO trends for each 5° x 5° grid cell between 80° S – 80° N, by season (DJF – top left, MAM – top right, JJA – bottom left, SON – bottom right). Trends in this figure are based on least-squares linear regression and reported with 95% confidence intervals and p-values. White dots indicate grid cells with statistically significant trends.

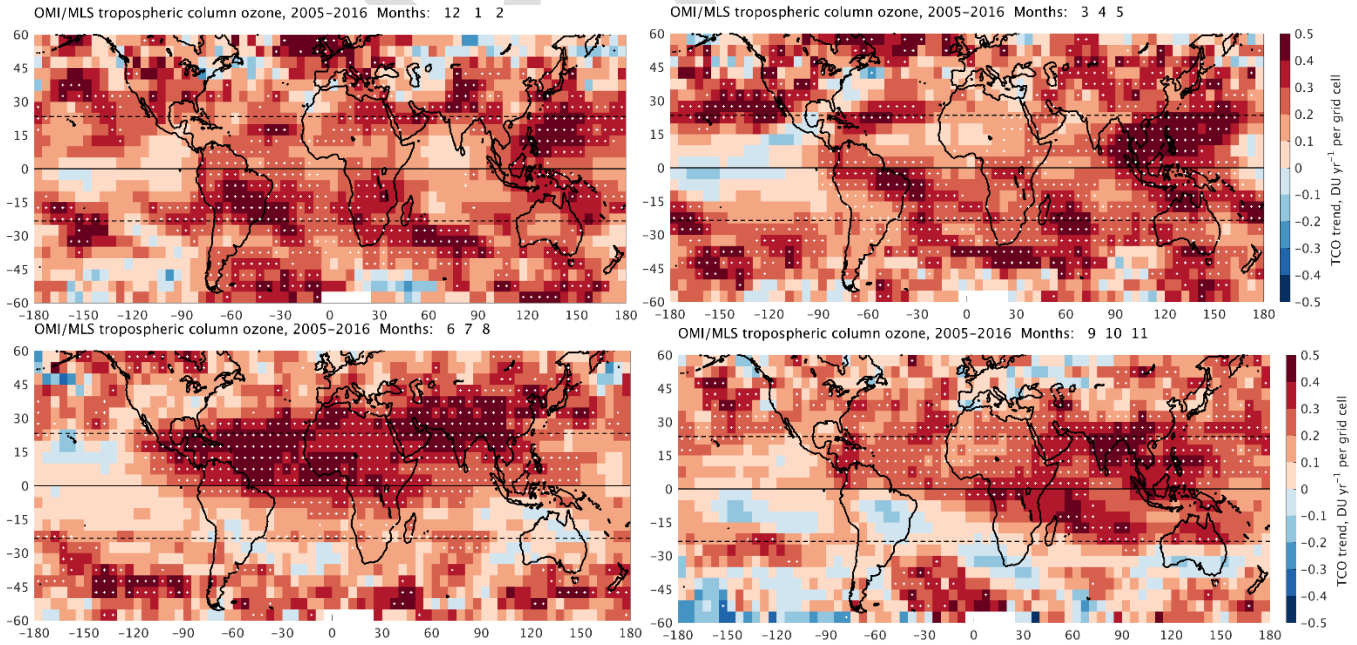

Figure S4.3.2. 2005-2016 OMI/MLS TCO trends for each 5° x 5° grid cell between 60° S – 60° N, by season (DJF – top left, MAM – top right, JJA – bottom left, SON – bottom right). White dots indicate grid cells with statistically significant trends.

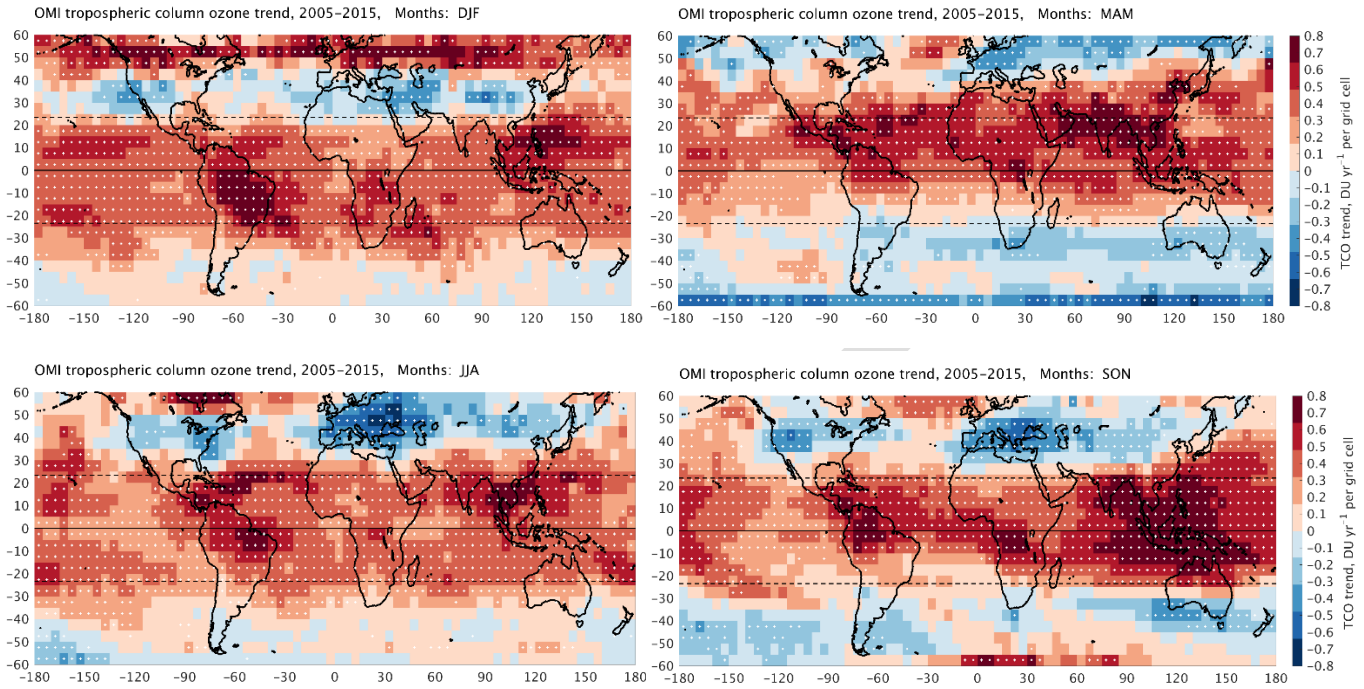

Figure S4.3.3. 2005-2015 OMI-SAO TCO trends for each 5° x 5° grid cell between 60° S – 60° N, by season (DJF – top left, MAM – top right, JJA – bottom left, SON – bottom right), after removing time-dependent systematic biases shown in Figure S.1. White dots indicate grid cells with statistically significant trends.

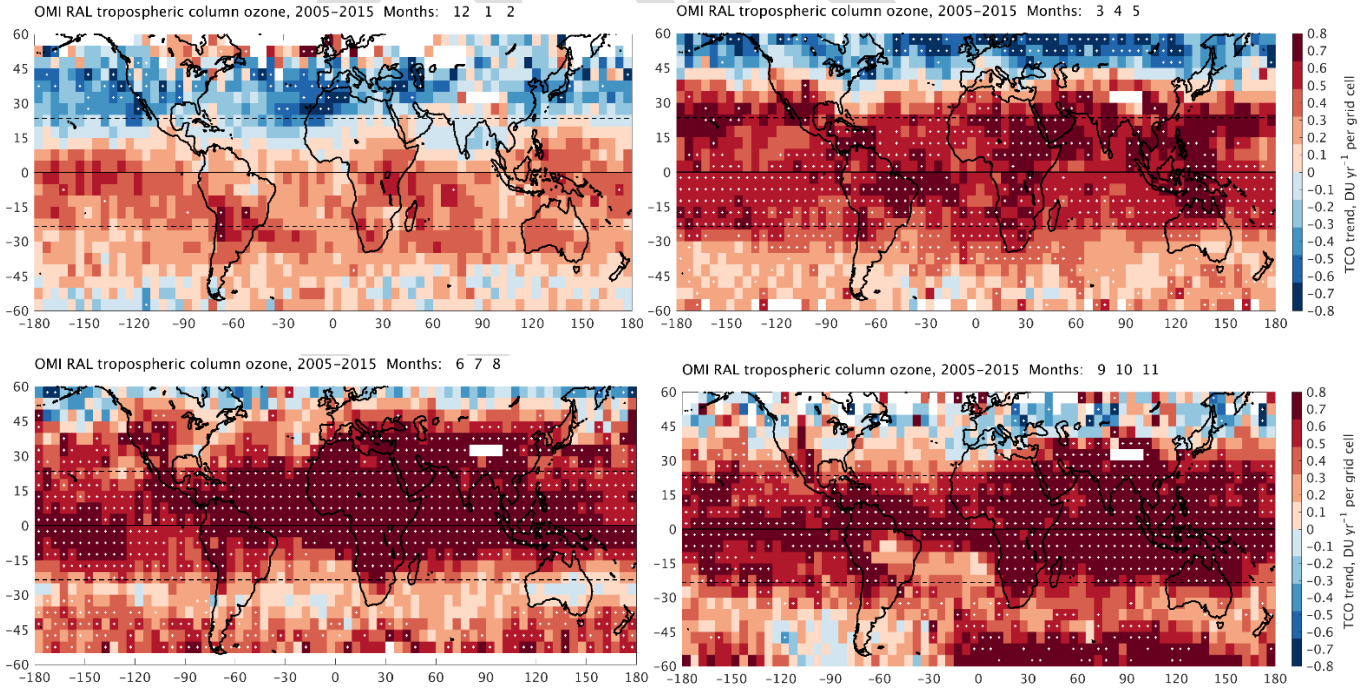

Figure S4.3.4. 2005-2015 OMI-RAL TCO trends for each 5° x 5° grid cell between 60° S – 60° N, by season (DJF – top left, MAM – top right, JJA – bottom left, SON – bottom right). White dots indicate grid cells with statistically significant trends.

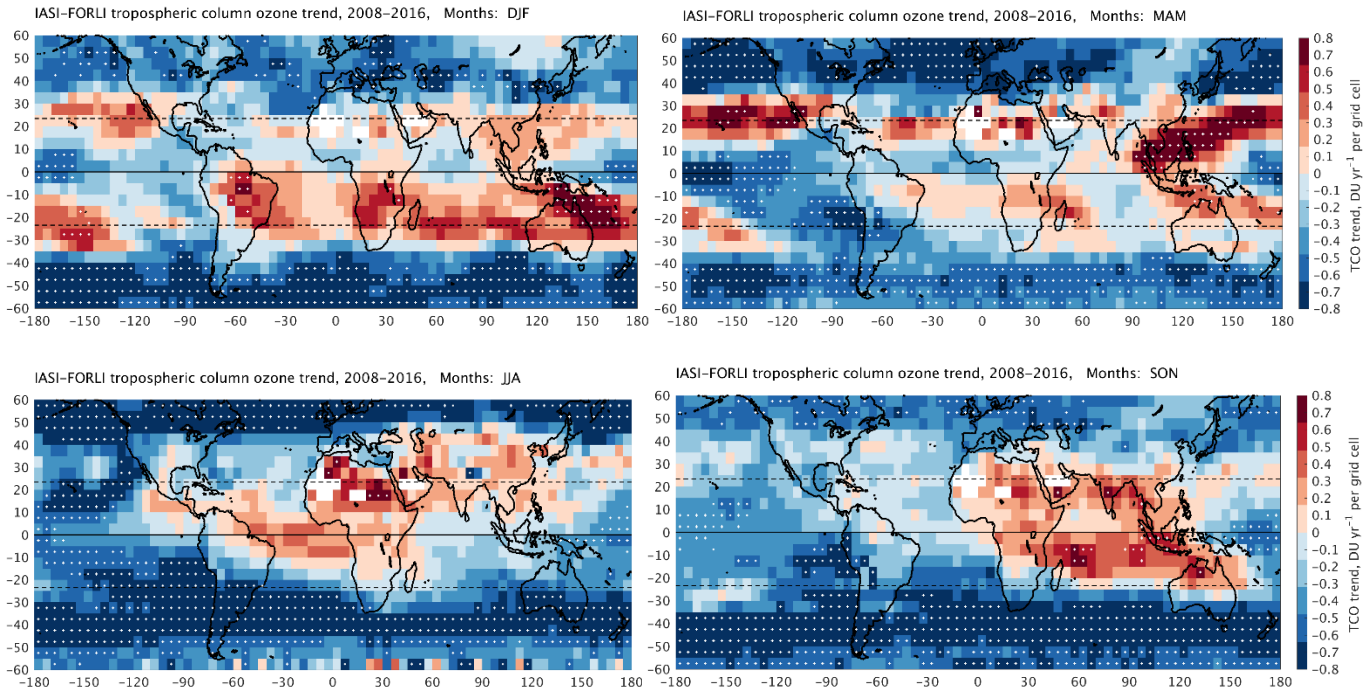

Figure S4.3.5. 2008-2016 IASI-FORLI TCO trends for each 5° x 5° grid cell between 60° S – 60° N, by season (DJF – top left, MAM – top right, JJA – bottom left, SON – bottom right). White dots indicate grid cells with statistically significant trends.

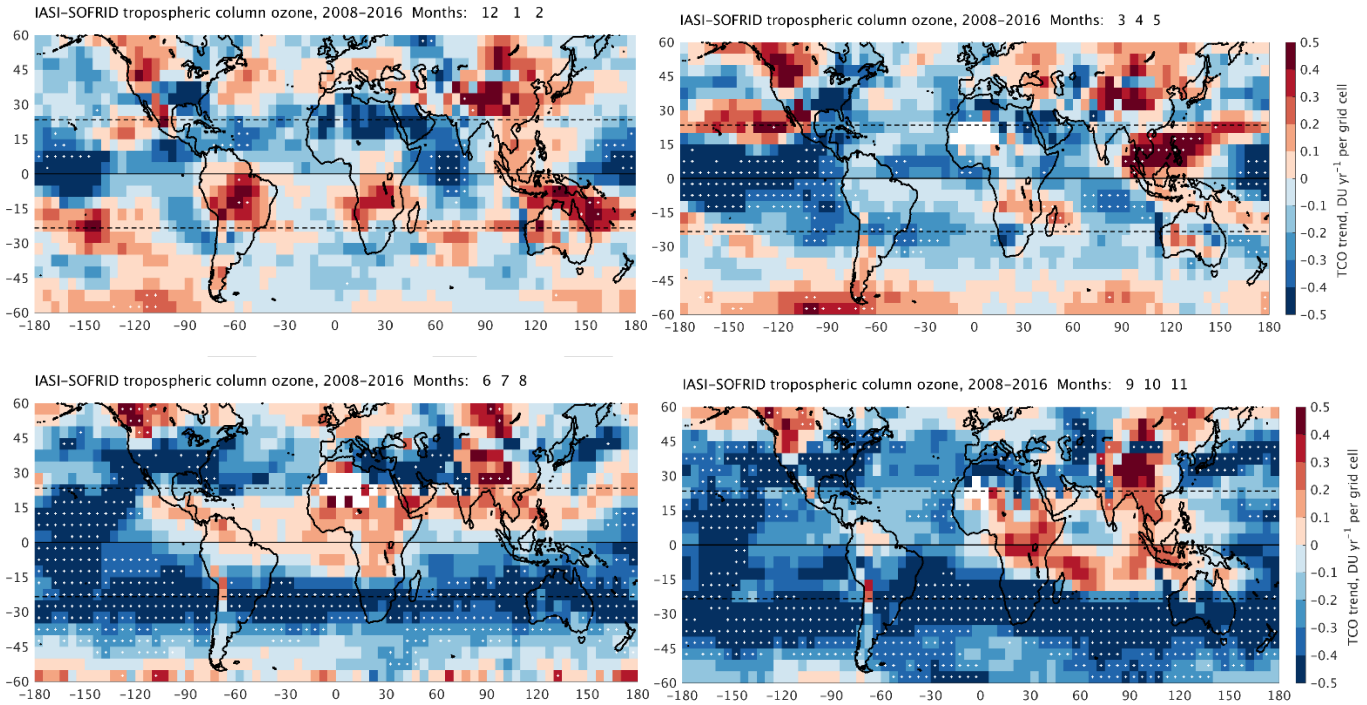

Figure S4.3.6. 2008-2015 IASI-SOFRID TCO trends for each 5° x 5° grid cell between 60° S – 60° N, by season (DJF – top left, MAM – top right, JJA – bottom left, SON – bottom right). White dots indicate grid cells with statistically significant trends.

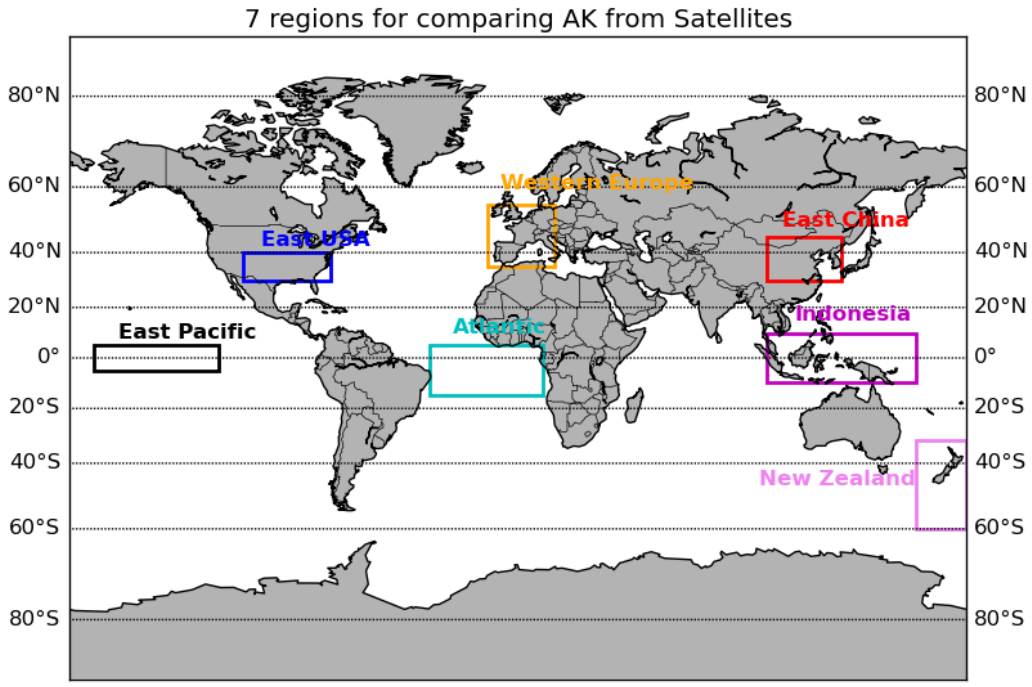

Figure S5.7.1. Map of the seven regions: East USA, East China, Atlantic, Indonesia, East Pacific, Western Europe, New Zealand, where are compared Averaging Kernels from five satellite products: OMI-MLS, OMI-SOA, OMI-RAL, IASI-SOFRID and IASI-FORLI (see figures S5.7.2 and S5.7.3).

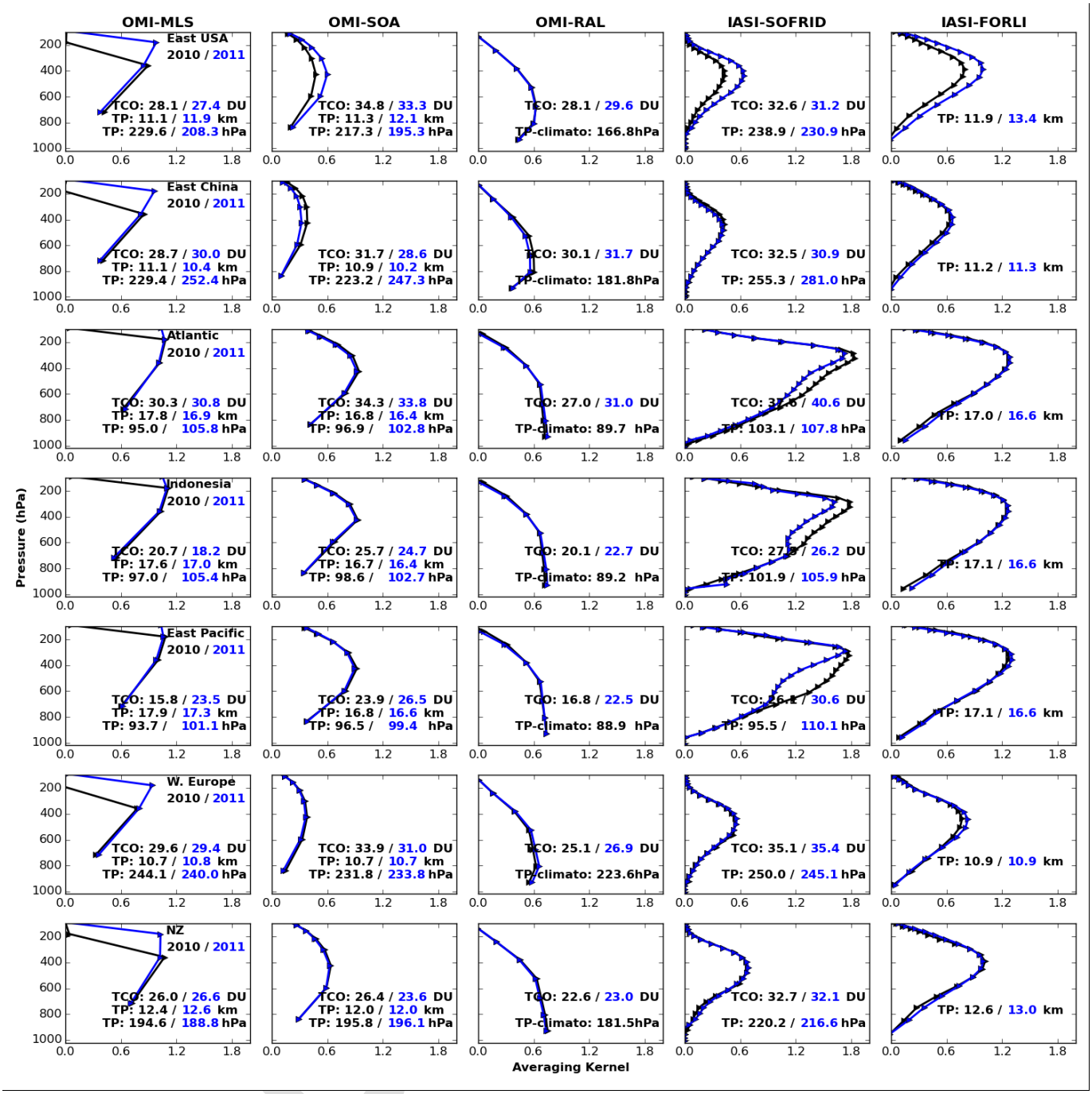

Figure S5.7.2. Comparison of Averaging Kernels from five satellite products: OMI-MLS, OMI-SOA, OMI-RAL, IASI-SOFRID and IASI-FORLI, for seven regions: East USA, East China, Atlantic, Indonesia, East Pacific, Western Europe, New Zealand (see figure S5.7.1), for the season December-January-February 2010 (black), 2011 (blue). The tropospheric ozone column (TCO) in Dobson Units (DU) and the tropopause height (TP) in hPa and/or in km was added to the figures.

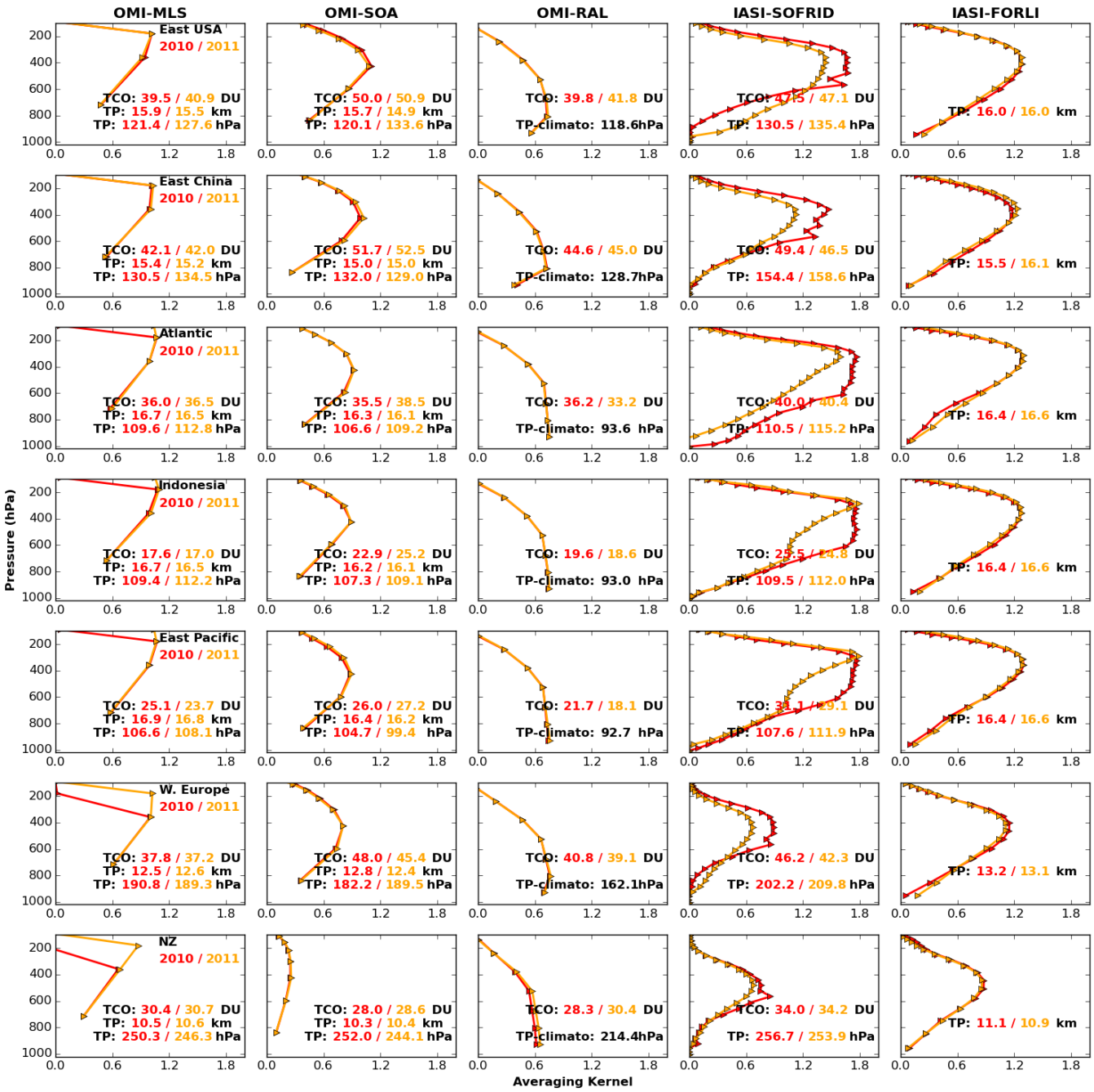

Figure S5.7.3. Same as figure S5.7.2 but for the season June-July-August.

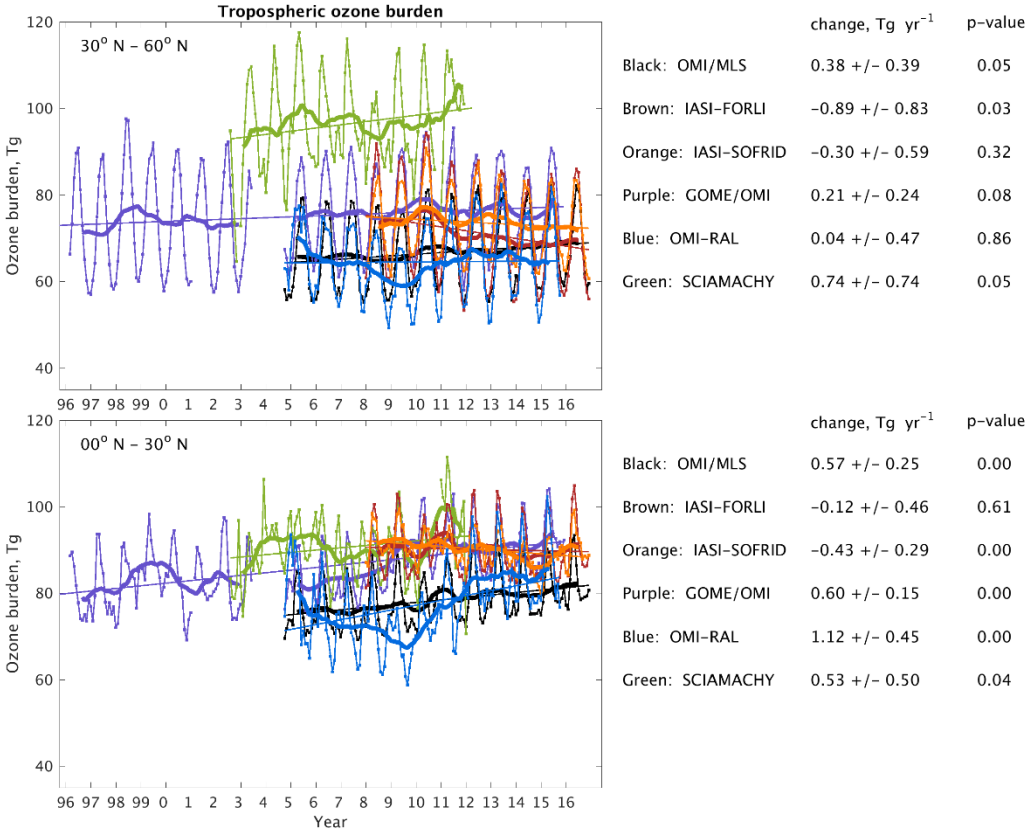

Figure S5.7.4. Northern Hemisphere monthly tropospheric ozone burden (thin curves) for 30° N - 60° N (top), and 0° - 30° N (bottom), for 6 different satellite products. Thick curves are the 12-month running means and the thin straight lines are the least square linear fits. Trends in this figure are based on least-squares linear regression and reported with 95% confidence intervals and p-values.

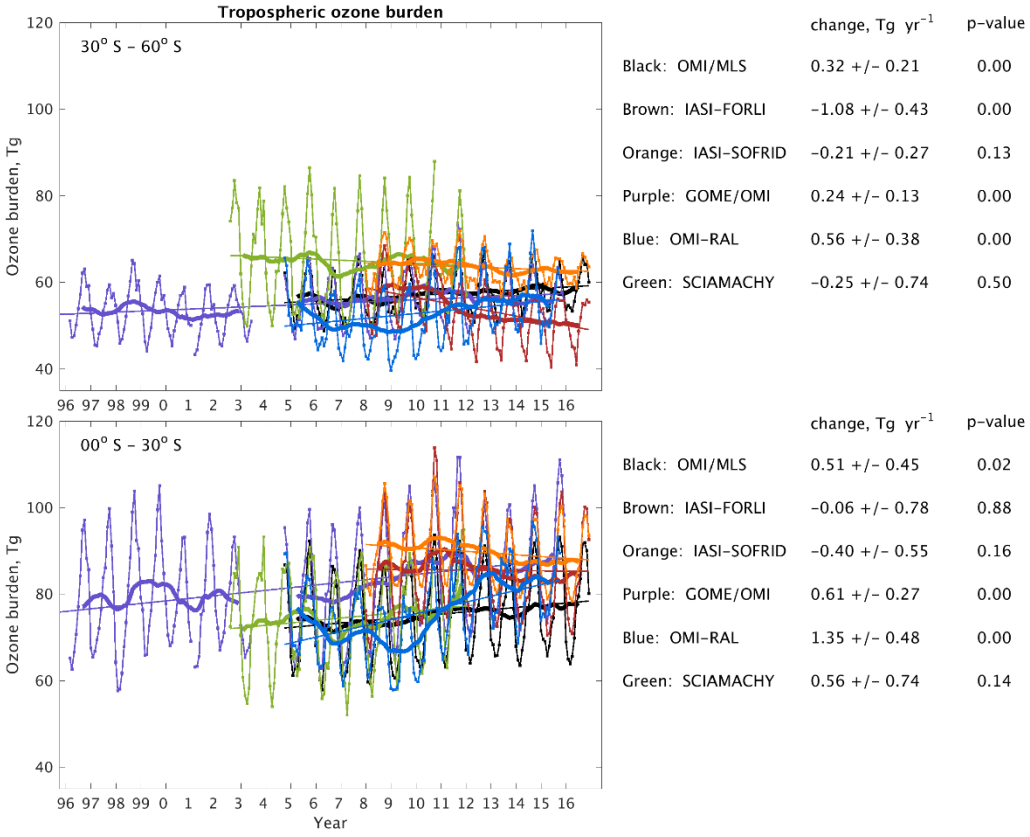

Figure S5.7.5. As in Figure S5.7.4 but for the Southern Hemisphere.